NUMERICAL STUDY ON THE CHLORIDE INDUCED STEEL CORROSION IN CONCRETE

C. Y. Kim (1) and J. K. Kim (2)

(1) Samsung Engineering, Korea

(2) Korea Advanced Institute of Science and Technology, Korea

Abstract

Three-dimensional finite element program which can perform the analyses of moisture transport, chloride attack, and steel corrosion simultaneously are developed. Each aspect is analyzed separately and successively, from the moisture transport to the steel corrosion, in order to simplify the analysis procedure and save the calculation time. Analysis priority for each aspect is determined from its influence to the other aspects, thereby the analysis error caused by ignoring the coupling effect can be minimized. After verifying the applicability of developed analysis program by performing a simulation analysis of Schieβl's experiment, a model analysis was made in order to determine the critical parameter which governs the rate of steel corrosion at the crack in RC structures. Analysis results revealed that the resistance of concrete is the most important parameter which determines the corrosion acceleration near the crack.

1. INTRODUCTION

Owing to recent numerical studies on steel corrosion in concrete, it is well documented that the fundamental theories of electrochemistry can be successfully applied to reinforced concrete (RC) structures for the evaluation of steel corrosion [1-4]. While research to date has yielded valuable insights, most of the existing researches on this subject are performed independently from the analysis of chloride attack. Since it is obvious that the steel corrosion behaviour is closely related to chloride attack, these aspects should be considered together in the same time and space domain in order to estimate the real nature of steel corrosion in concrete accurately. The limited applicability to one- or two-dimensional structures is another problem of existing researches. In order to deal with some special but frequently facing problems, e.g. RC structures having cracks or macro-cell corrosion problem, the applicability of analysis should be extended to three-dimensional (3D) cases.

In this study, 3D finite element program which can perform the analyses of moisture transport, chloride attack, and steel corrosion simultaneously are developed and, in addition to

this, the verification analysis and model study are made to confirm its applicability and to numerically investigate a practical situation.

2. ANALYSIS METHOD

2.1 Moisture transport analysis

Assuming that the moisture transport in concrete is isotropic and the self desiccation due to hydration of concrete is negligible, the governing equation of moisture transport, which describes the time dependent variation of moisture distribution in concrete, is expressed as follows:

$$\frac{\partial(RH)}{\partial t} = D_w \nabla^2 (RH) \tag{1}$$

where RH is relative humidity, t is time, D_w is diffusivity of humidity, and ∇^2 is Laplacian operator.

2.2 Chloride attack analysis

Based on the diffusion theory and the mass conservation considering the binding and the convective flow of chloride ion, the governing equation for the penetration of chloride ion can be derived as follows [4]:

$$\left(\frac{\partial C_b}{\partial C_f} + pS \right) \frac{\partial C_f}{\partial t} = \nabla [pSD_{Cl} \nabla C_f] + pC_f \frac{\partial S}{\partial t} \tag{2}$$

where C_b and C_f is bound and free chloride concentration, p is porosity of concrete, S is degree of pore saturation, and D_{cl} is diffusivity of chloride ion. The second term in the right side represents the convective flow of chloride ion due to moisture transport. The rate of moisture change ($=\partial S/\partial t$) can be calculated from the result of humidity analysis and the sorption isotherm. The binding capacity term ($=\partial C_b/\partial C_f$) in the left side is approximately estimated from the previously calculated concentration of free chloride [4].

2.3 Corrosion analysis

If the electrical resistance of concrete is assumed to be isotropic, the distribution of electric potential is governed by Laplace's equation.

$$\nabla^2 \phi = 0 \tag{3}$$

where ϕ is electric potential. To obtain the potential distribution in concrete, the solution of Equation (3) subjected to the natural boundary conditions derived from Ohm's law and electrochemical equations should be found [2, 4]; unfortunately, this problem cannot be solved explicitly since the imposed boundary value is dependent on the potential, i.e. the solution of Equation (3). Additionally, an essential boundary condition should be imposed manually since a unique solution cannot be obtained solely from the natural boundary conditions. In order to deal with these problems, a solution strategy including some iteration procedures was developed by the authors [2, 4].

2.4 Analysis procedure

On the basis of governing equations described in the previous sections, 3D finite element program which can perform the analyses of moisture transport, chloride attack, and steel

corrosion in the same time and space domain are developed. Although the coupling effect among these aspects can best be investigated by means of iteration method, each aspect is analyzed separately and successively, from the moisture transport to the steel corrosion, in order to simplify the analysis procedure and save the calculation time. Figure 1 illustrates the integrated analysis procedure. Analysis priority for each aspect is determined from its influence to the other aspects, thereby the analysis error caused by ignoring the coupling effect can be minimized. For instance, greatest priority is given to moisture transport analysis because it affects all the other aspects as depicted in Figure 1.

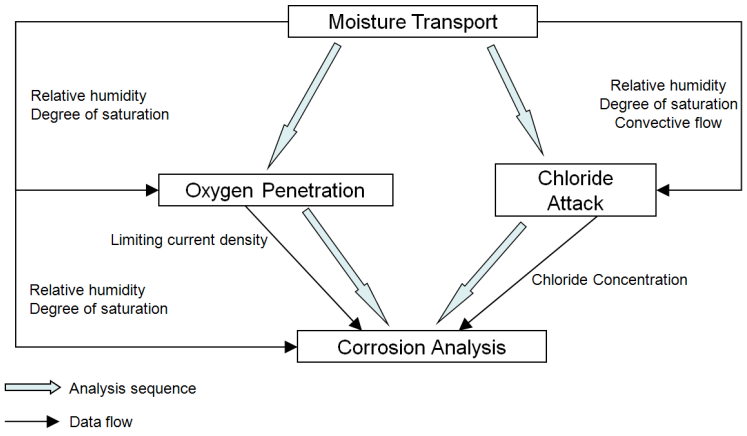

Figure 1: Analysis procedure

3. VERIFICATION ANALYSIS

Since it is apparent that the rate of steel corrosion is highly accelerated if steel is directly exposed to external environment through cracks, many research effort have been devoted to clarify the influence of crack on the steel corrosion [5-7]. According to those researches, the rate of corrosion can be accelerated up to 3~7 times faster near crack even for the RC structures having high quality of concrete cover. In the cracked RC structures, anodic reaction mainly takes place at the surface of steel located near crack while the other part of steel surface serves as a cathode. Therefore, reasonable estimation of macro-cell corrosion current is essential for the accurate estimation of steel corrosion behavior in cracked RC members.

Figure 2 schematically describes the Schieβl et al.'s experimental setup [5]. In his experiment, steel bar is segmented into seven pieces to prevent the electron transfer between each segment and they are connected indirectly by using a conductive wire to measure macro-cell corrosion currents. As depicted in the figure, crack is intentionally made through the centrally located steel segment and 1 percent chloride solution is imposed through the crack, for 1 day/week periodically, to induce active corrosion. Water-cement ratio and unit cement content for the concrete were 0.6 and 300 kg/m^3, respectively. The specimens are stored under the controlled environment where the relative humidity is 80% and the temperature is 20 ^{o}C. Figure 3 shows a finite element (FE) mesh constructed for the verification analysis. Surfaces indicated by red color represent the steel surfaces where natural boundary conditions for steel corrosion are imposed. As shown in the figure, boundary conditions are not imposed at the separated region between each steel segment to reproduce the actual experimental setup. For the proper estimation of corrosion behavior, some material parameters are manually determined and those are summarized in Table 1.

Figure 4 compares the time history of macro-cell corrosion current reported in the experiment and that calculated from the corrosion analysis. At the early stage of exposure, measured macro-cell corrosion current shows a strong oscillation. The amplitude of oscillation is gradually decreasing as the increase of exposing time. It is interesting that the numerically calculated corrosion current also shows similar oscillating behavior; its amplitude is largest at the beginning of exposure and gradually decreases. According to the analysis result, the reason for the strong oscillation at the early stage is that the depassivated area of steel is periodically changing with the cyclic variation of boundary condition, i.e. with cyclic wetting and drying. And the gradual decrease of the oscillation amplitude is attributed to the decrease in the relative variation of depassivated area due to the clclic wetting and drying. Change in polarization property due to direct contact of chlorides with steel surface, and faster mass transport through the porous transition zone at the interface between steel and concrete could be additional reasons which can explain the relatively larger oscillation observed in the experimental result. Since the duration for the sharp increase in corrosion current observed in the experiment is relatively short, it can be concluded that the calculated corrosion current describes the overall corrosion behavior observed in the experiment quiet reasonably.

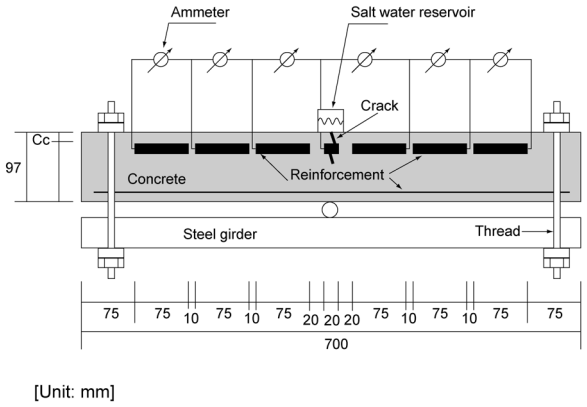

Figure 2: Test setup (Schieβl et al.)

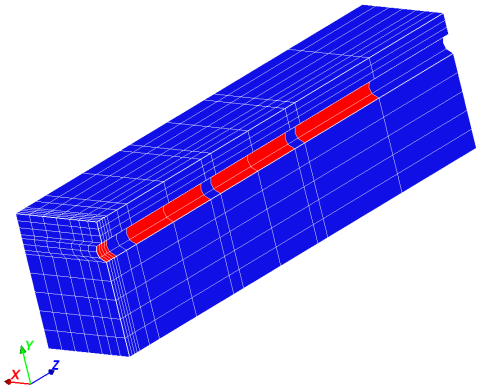

Figure 3: FE mesh for the analysis

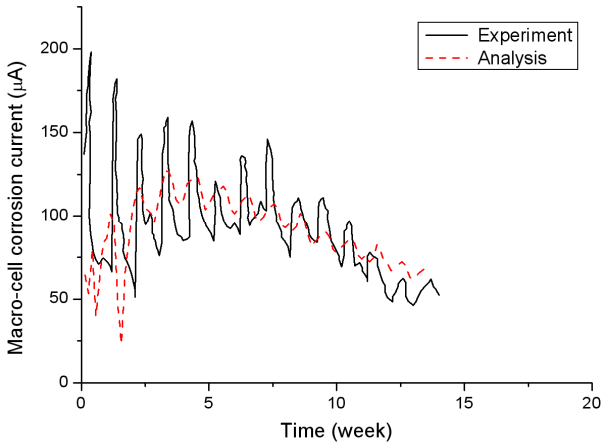

Figure 4: Macro-cell corrosion current history

Table 1: Input data for the verification analysis

Material parameter	Value
Threshold concentration of chlorides (kg/m^3 solution)	5
External oxygen concentration (kg/m^3 solution)	0.0085
Cathodic exchange current density (A/cm^2)	6×10^{-10}
Cathodic equilibrium potential (mV vs. SCE)	160
Anodic exchange current density (A/cm^2)	2.75×10^{-8}
Anodic equilibrium potential (mV vs. SCE)	690
Aging factor	0.55

4. MODEL STUDY

In this section, a number of analyses are performed to investigate the influence of some essential parameters on the rate of steel corrosion at crack. Resistance of concrete, cover depth, spacing between cracks, and clear spacing between reinforcements are selected as essential parameters. Values of the parameters used for the model study are summarized in Table 2. Other electrochemical properties used are the same as those described in Table 1. Water/cement ratio is assumed to be 0.5. Figure 5 describes the simulated situation for the model study. As shown in the figure, the diameter of reinforcement steel is fixed to be 20 mm and the length of depassivated area is limited to be 10 mm.

Table 3 summarizes the analysis results, which confirms that the rate of corrosion is significantly accelerated at locally depassivated steel surface; cf. the rate of active corrosion for uncracked RC member is usually 1~3 $\mu A/cm^2$ [8]. This aspect is mainly attributed to the additional contribution of large scale macro-cell corrosion. Also, it can be observed that the calculated rates of steel corrosion for the resistance of 800 ohm m are almost constant regardless of the difference in geometric parameters, while those for the resistance of 50 ohm m show considerable variations. It seems that the geometric condition has little influence on the acceleration of corrosion rate at crack for high quality concrete.

To clearly see the influence of each parameter, calculated corrosion current densities are normalized with the current densities calculated for the standard values. The normalized values, denoted as relative corrosion current density, are displayed in Figure 6. As shown in Figure 6(a), resistance of concrete strongly affects the rate of steel corrosion at crack; the rate of corrosion is doubled if the resistance of concrete is reduced to quarter of its original value. Figure 6(b) shows that the spacing between cracks also has some influence on the rate of steel corrosion. However, the influence is decreasing as the increase of resistance; it is fairly predictable since the available steel surface which serves as cathode reduces as the resistance of concrete increases. Incidentally, as shown in Figures 6(c) and 6(d), cover depth and clear spacing have little influence on the rate of steel corrosion at crack.

From the results derived from the model study, it can be conclude that the rate of steel corrosion can be restricted under properly low level even for the cracked RC members if the resistance of concrete, i.e. quality of concrete, is sufficiently high. Also, it is envisaged that increasing the cover depth is not useful way for the control of corrosion rate at crack, though

it may prevent the crack from passing through the steel. Consequently, if one wants to improve the corrosion resistance as well as the service life of RC structures, it is more beneficial to improve the quality of cover concrete rather than to increase the cover depth only.

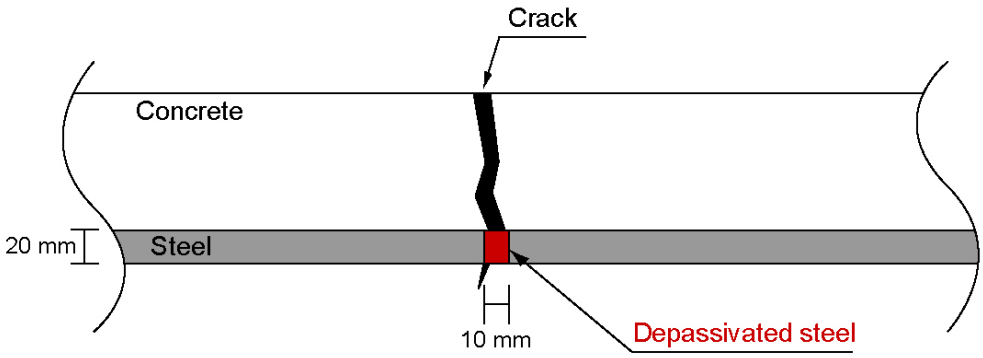

Figure 5: Simulated situation for the model study

Table 2: Input data for the model study

Parameter	Value
Cover depth (mm)[a]	30, 60, 120
Spacing between cracks (mm)[a]	200, 500, 1000
Clear spacing between reinforcements (mm)[a]	100, 300
Electrical resistance of concrete (Ohm m)[a]	50, 200, 800

[a] Underlined value is the standard value for each parameter.

Table 3: Calculated corrosion current density

Resistance (Ohm m)	Geometry [a]	Corrosion current density (μA/cm^2)
50	30-500-300	20.8
	60-200-300	15.0
	60-500-100	20.1
	60-500-300	20.9
	60-1000-300	25.9
	120-500-300	20.6
200	30-500-300	11.0
	60-200-300	8.77
	60-500-100	10.4

	60-500-300	10.9
	60-1000-300	12.3
	120-500-300	10.6
800	30-500-300	5.44
	60-200-300	4.57
	60-500-100	4.68
	60-500-300	5.12
	60-1000-300	5.42
	120-500-300	4.77

[a] Each geometry name is defined as [cover depth (mm)]–[spacing between cracks (mm)]–[clear spacing between reinforcements (mm)].

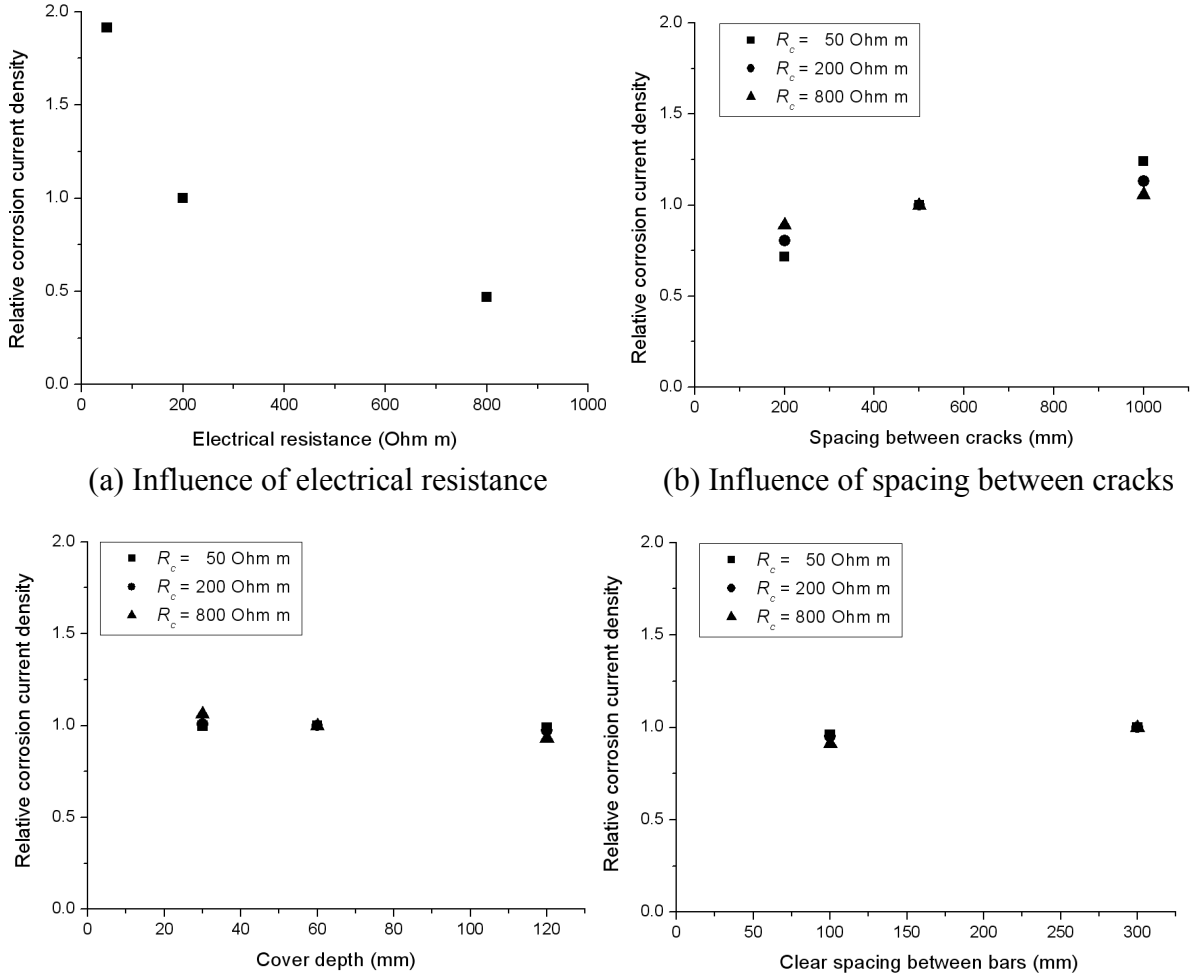

(a) Influence of electrical resistance (b) Influence of spacing between cracks

(c) Influence of cover depth (d) Influence of clear spacing between bars

Figure 6: Influence of selected parameters on the relative corrosion current

5. CONCLUSIONS

- Three dimensional finite element program which can perform the analyses of moisture transport, chloride attack, and steel corrosion simultaneously are developed. Each aspect is analyzed separately and successively in order to simplify the analysis procedure and save the calculation time. Analysis priority for each aspect is determined from its influence to the other aspects, thereby the analysis error caused by ignoring the coupling effect can be minimized.
- A simulation analysis of Schieβl's experiment was performed in order to verify the applicability of developed analysis program. The results show that the calculated corrosion current describes the overall corrosion behavior observed in the experiment quiet reasonably.
- Model analysis was made in order to determine the critical parameter which governs the rate of steel corrosion at the crack in RC structures. Analysis results revealed that the resistance of concrete is the most essential parameter which determines the corrosion acceleration near the crack. Therefore, if one wants to improve the corrosion resistance as well as the service life of RC structures, it seems to be more beneficial to improve the quality of cover concrete rather than to increase the cover depth only

ACKNOWLEDGEMENTS

This research was supported by a grant (07 High Tech A01) from High Tech Urban Development Program and a grant (No. 2009-0063550) from National Research Foundation of Korea (NRF), both funded by Korean government.

REFERENCES

[1] Isgor, O. B. and Razaqpur, A. G., 'Modeling steel corrosion in concrete structures', *Materials and Structures*, **39** (3) (2006) 291-302.
[2] Kim, C. Y. and Kim, J. K., 'Numerical analysis of localized steel corrosion in concrete', *Construction and Building Materials*, **22** (6) (2008) 1129-1136.
[3] Kranc, S. C. and Sagüés, A. A., 'Detailed modeling of corrosion macrocells on steel reinforcing in concrete', *Corrosion Science*, **43** (7) (2001) 1355-1372.
[4] Kim, C. Y., 'Numerical study on steel corrosion in concrete exposed to carbonation and chloride attack', Ph. D. Thesis, Korea Advanced Institute of Science and Technology, (2008)
[5] Schieβl, P. and Raupach, M., 'Laboratory studies and calculations on the influence of crack width on chloride-induced corrosion of steel in concrete', *ACI Materials Journal*, **94** (1) (1997) 56-62.
[6] Otsuki, N., Miyazato, S., Diola, N. B. and Suzuki, H., 'Influence of bending crack and water-cement ratio on chloride-induced corrosion of main reinforcing bars and stirrups', *ACI Materials Journal*, **97** (4) (2000) 454-464.
[7] Mohammed, T. U., Otsuki, N., Hisada, M. and Shibata, T., 'Effect of crack width and bar types on corrosion on steel in concrete', *Journal of Materials in Civil Engineering*, **13** (3) (2001) 194-201.
[8] González, J. A., Andrade, C., Alonso, C. and Feliu, S., 'Comparison of rates of general corrosion and maximum pitting penetration on concrete embedded steel reinforcement', *Cement and Concrete Research*, **25** (2) (1995) 257-264.